The Journal of Experimental Biology 211, 3594-3600
Published by The Company of Biologists 2008
doi:10.1242/jeb.021923

FRAP analysis of molecular diffusion inside sea-urchin spermatozoa

Daisuke Takao and Shinji Kamimura*

Department of Life Science, Graduate School of Arts and Sciences, The University of Tokyo, Komaba 3-8-1, Meguro, Tokyo 153-8902, Japan

*Author for correspondence at present address: Department of Biological Sciences, Faculty of Science and Engineering, Chuo University, Kasuga 1-13-27, Bunkyo-ku, Tokyo 112, Japan (e-mail: kam@myad.jp)

Accepted 18 September 2008

SUMMARY

In sea-urchin spermatozoa, energy required for flagellar motility is provided by ATP diffusion from mitochondria located at the proximal ends of the flagella along with the creatine shuttle system. However, no direct analysis of the diffusion rates inside flagella has been carried out thus far. Using a FRAP (fluorescence recovery after photobleaching) technique, we determined the diffusion coefficients of fluorescein-derivatives (calcein, carboxyfluorescein and Oregon Green) to be 63–64 $\mu m^2 s^{-1}$. Although these values are about one third of the estimates that were previously used for theoretical calculations, we concluded that the rate of ATP diffusion inside spermatozoa was high enough to support the continuous motility of sea-urchin sperm flagella if the creatine shuttle system is working. We also investigated the diffusion rate through the 'neck' region between the head and tail. When the head region of a calcein-loaded spermatozoon was photobleached, slow recovery of head fluorescence along with the decrease of fluorescence signal in the tail region was observed. It suggests that small molecules such as calcein (M_r, 622.54) can move beyond the boundary between the head and the flagellum. We expect that these findings regarding the diffusion properties inside spermatozoa will provide us with more general insights into the energy equilibrium and material transportation by passive diffusion inside eukaryotic cilia and flagella.

Key words: FRAP, diffusion constants, intra-flagellar transport, molecular mobility.

INTRODUCTION

The movement of sperm flagella is driven by microtubule sliding powered by dynein arms, which is coupled to ATP hydrolysis. In the case of sea-urchin spermatozoa, respiration by the mitochondria located at the flagellar basal ends is the main source of ATP. Besides free diffusion of ATP along the flagella to the tip ends, energy is also provided by phosphocreatine (PCr) using a creatine shuttle system (Tombes and Shapiro, 1985). So far, several reports have been presented (Brokaw, 1966; Nevo and Rikmenspoel, 1970; Tombes et al., 1987) showing theoretical simulations of energy transportation along beating flagella. However, these studies used the diffusion coefficients of ATP or PCr, obtained in aqueous solution (Brokaw, 1966; Nevo and Rikmenspoel, 1970) or in muscle fibers (Tombes et al., 1987), because no appropriate data acquired by the direct analysis of diffusion was available. Since the cytoplasmic space inside the flagellum is largely occupied by the structural components of axonemes (Nicastro et al., 2005), apparent molecular mobility under such crowded conditions might be severely restricted compared with that in typical cell cytoplasm. Hence, direct studies on diffusion rates have been expected to elucidate such detailed features.

Fluorescence recovery after photobleaching (FRAP) has been established as a method to determine the diffusion coefficients in live cells (Ladha et al., 1994; Wey and Cone, 1981; Yguerabide et al., 1982). In FRAP, a small region of interest is photobleached by a laser pulse and diffusion coefficients can be determined by measuring the time course of fluorescence recovery. In the current work, we performed FRAP experiments to determine the apparent diffusion coefficients of small fluorescent probes, calcein, carboxyfluorescein and Oregon Green in both flagella and aqueous solutions. These results provide the first direct determination of intra-flagellar diffusion rates.

The second area of interest was diffusion and material transportation between head and flagellum. During the activation of motility and the preparation for fertilization, spermatozoa undergo a sequential change of the concentrations of ions and signaling messengers that function as essential cue chemicals affecting the flagellar motility and acrosomal reactions (Darszon et al., 2001). It is therefore likely that, for these ions and signals to work at an exact place and time, they are compartmentalized in a specific region in spermatozoa. By electron microscopy the 'neck' region between head and flagellum was shown to be densely packed in mammalian sperm (Pessh and Bergmann, 2006). In addition, the presence of diffusion barriers has been reported in the plasma membrane of mammalian sperm (James et al., 2004; Ladha et al., 1997; Mackie et al., 2001). Such evidence suggests that there could be an intracellular diffusion barrier around the neck region. Although recent detailed information on the active intra-flagellar transport (IFT) systems along cilia and flagella revealed their critical roles in the structural and functional maintenance of axonemes (Rosenbaum and Witman, 2002), another possible path of material diffusion beyond the neck region has not been described. We analyzed fluorescence recovery in the head region of sperm and investigated whether the molecular mobility through the neck region is restricted.

MATERIALS AND METHODS

Materials

Chemicals were purchased from the following suppliers unless otherwise stated: Wako (Osaka, Japan), Sigma-Aldrich Japan (Tokyo), or Dojindo (Kumamoto, Japan). Fluorescent probes (calcein, carboxyfluorescein and Oregon Green) and their acetoxymethyl (AM) or diacetate (DA) esters were obtained from

Invitrogen (Carlsbad, CA, USA). We chose these fluorescent dye species because they can be incorporated into sperm cells by incubation, and they have molecular masses similar to that of ATP. Calcein, carboxyfluorescein and Oregon Green were prepared as 20 mmol l^{-1} DMSO stock solutions and kept at –20°C before use. Calcein-AM, carboxyfluorescein-DA, and Oregon Green-DA were stored as 2.5, 20 and 4.0 mmol l^{-1} DMSO stock solutions, respectively, at –20°C.

Spawned sperm from sea urchin, *Pseudocentrotus depressus* A. Agassiz, were obtained by intracoelomic injection of 0.5 mol l^{-1} KCl. Collected sperm (dry sperm) were stored without dilution at 4°C until use. Artificial sea water (ASW) containing 460 mmol l^{-1} NaCl, 10 mmol l^{-1} KCl, 23 mmol l^{-1} $MgCl_2$, 0.1 mmol l^{-1} EDTA, 10 mmol l^{-1} $CaCl_2$ and 10 mmol l^{-1} MES (pH 6.0) or 10 mmol l^{-1} HEPES (pH 7.0) was used as the experimental medium.

Loading of fluorescent probes into sea-urchin spermatozoa

In order to load fluorescent probes into sea urchin spermatozoa, we used the method previously described by Rodriguez and Darszon (Rodriguez and Darszon, 2003) with some modifications. Sperm were loaded with fluorescent probes by diluting 20 µl of dry sperm with 100 µl of ASW (pH 6.0) containing 20 µmol l^{-1} AM or DA esters of fluorescent probes for 4 h at 4°C in the dark. After the loading of probes, the remaining probes in the medium were removed by centrifugation (2000 ***g***, 3 min, 4°C). The collected pellet of sperm was resuspended in 200 µl ASW (pH 6.0). The washing procedure was repeated twice. The sperm pellet was finally suspended in 100 µl ASW (pH 6.0) and kept on ice until use.

Fluorescence recovery after photobleaching analysis

For the observation of conventional fluorescence images, an epifluorescence microscope (IX-70; Olympus, Tokyo, Japan) with an Olympus U-MSWB filter-set (for green fluorescence observations) was used. Specimens were observed under the continuous illumination of a high-pressure mercury lamp. To avoid the photobleaching of fluorescent probes, the mercury lamp light source was attenuated with ND filters. Fluorescence images through an emission filter were amplified with an image intensifier (C7787; Hamamatsu Photonics, Hamamatsu, Japan) and collected on to a computer with a high speed CCD camera system (HAS-200R; Ditect, Tokyo) at 200 f.p.s. Under these conditions, the rate of photobleaching during image observation was low ($\tau_{1/2}$ ~30 s) compared with the FRAP rates (~2 s for full recovery) of dyes we used.

For the photobleaching experiments of fluorescent probes, a 488 nm argon laser (5500ASL; DZ Laser Service, Centerville, UT, USA) was used. The laser beam was introduced into the microscope optics through an objective (UApo/340 ×40/1.35 oil immersion lens; Olympus, Tokyo, Japan) by reflection using a small rod mirror placed on the microscope optical axis just below the objective. The intensity profile of the focused laser spot on the specimen field was measured with the CCD camera and fitted to a Gaussian distribution, which gave a spot radius parameter, ω, of 3.05 µm ($1/e^2$). The intensity and exposure time of bleaching laser pulses were modulated with ND filters as well as a mechanical shutter (EC-598; Copal, Tokyo, Japan). The mechanical shutter was controlled with a shutter driver (EN-609; Copal, Tokyo, Japan) and a hand-made circuit using timer integrated circuits (LM555CN/NOPB; National Semiconductor, Santa Clara, CA, USA). We also made the shutter controller to switch off the image intensifier during photobleaching to avoid damages by the high intensity illumination of the argon laser.

Spermatozoa that had been pre-loaded with fluorescent probes were diluted with ASW (pH 7.0) and placed in a chamber made of two coverslips separated with a pair of stripped plastic tape spacers. Spermatozoa were attached to the glass surfaces of coverslips and we used such spermatozoa for further observations. The specimen was then washed with 200 µl of ASW (pH 7.0) to remove remaining dye and free spermatozoa in the solution. To determine the diffusion coefficients in aqueous solutions by the FRAP experiments, 4 µl of experimental solutions containing 10 mmol l^{-1} HEPES (pH 7.0), 20–60% (v/v) glycerol, and 20 µmol l^{-1} fluorescent dye were placed between two coverslips without plastic tape spacers. In these cases, observed diffusion is two-dimensional. We used ImageJ (NIH, Bethesda, MD, USA) to determine the intensity of fluorescence in recorded images. All the FRAP experiments were carried out at room temperature (20–23°C).

For data analysis, we first obtained time constants, $\tau_{1/2}$, by fitting the time courses of fluorescence recovery in photobleached regions to the following equation (Ladha et al., 1994; Yguerabide et al., 1982):

$$F(t) = \frac{F_0 + F_\infty(t / \tau_{1/2})}{1 + (t / \tau_{1/2})} , \quad (1)$$

where $F(t)$ is the fluorescence intensity at a time t. F_0 and F_∞ are the fluorescence intensities immediately after and at infinite time (>1 s) after the photobleaching, respectively. $\tau_{1/2}$ is the time required for the half recovery of fluorescence. For fitting data to the theoretical equations to obtain F_0, F_∞ and $\tau_{1/2}$, the least-square fitting algorithm programmed with Mathematica (ver. 5.0, Wolfram Research, Champaign, IL, USA) was used. D_x and D_{xy}, the diffusion coefficients for one-dimensional and two-dimensional diffusions, respectively, are given by the following expressions (Ladha et al., 1994; Wey and Cone, 1981):

$$D_x = \beta\omega^2 / 2\tau_{1/2} , \quad (2)$$

$$D_{xy} = \beta\omega^2 / 4\tau_{1/2} , \quad (3)$$

where β is the depth of the photobleaching parameter and ω is the half-width at $1/e^2$ intensity around the focusing point of the photobleaching laser beam. β varies depending on the percentage of dye photobleaching. We took β values ranging from 1.0–1.2 in our experiments depending on the magnitude of bleaching (signal ratios before *vs* after photobleaching) according to the theoretical estimation by Yguerabide and colleagues (Yguerabide et al., 1982).

Determination of head/flagellum volume ratio

By directing a photobleaching laser beam to the head region of spermatozoa, we were also able to photobleach fluorescent dye in the heads. If the amount of fluorescence recovery in the heads is equal to the loss in the flagellum, and the total fluorescence of the whole spermatozoon is constant, we can estimate the volume ratio of spaces fluorescent probes can access, $V_{head}/V_{flagellum}$, using the equation expressed by:

$$V_{head} / V_{flagellum} = (F_{f0} / F_{f\infty} - 1) / (1 - F_{h0} / F_{h\infty}) , \quad (4)$$

where F_{f0} and $F_{f\infty}$ are the total amounts of fluorescence in the flagellum immediately after and at infinite time after photobleaching, respectively. F_{h0} and $F_{h\infty}$ are the same parameters for heads (see Appendix for more details).

RESULTS

FRAP in flagella

By incubating sea-urchin spermatozoa in solutions of fluorescent probes for more than 4 h at pH 6.0, we found that the fluorescent signals incorporated into spermatozoa were bright enough for our

photobleaching experiments. Fig. 1 shows a typical example of fluorescence images before and after photobleaching. After repeated photobleaching in a restricted area of sperm tail, the fluorescence intensity of the whole spermatozoon, except for the acrosomal and mitochondrial regions, gradually decreased to a level almost comparable to the background noise. This indicates that the fluorescence probe molecules incorporated into the tail region of the sperm were not trapped or absorbed by any axonemal structural components and were almost free to move inside the spermatozoa, that is, there was apparently no immobile fraction. It is also clear that the fluorescence recovery we observed was not a spontaneous recovery of fluorescence photoemission after bleaching, but rather a demonstration of the apparent intracellular diffusion or mobility of fluorescent probes.

For quantitative analysis, we chose the photobleached area of ~6 μm in diameter corresponding to the focused region of laser beam in each recorded image and measured the mean fluorescence brightness (ImageJ, ver. 1.3). Each value normalized by the initial fluorescence intensity before photobleaching was plotted against time as shown in Fig. 2. All the fluorescein-derivatives we used in the experiments – calcein, carboxyfluorescein, and Oregon Green – showed similar recovery rates (Fig. 2A–C), although their molecular masses are slightly different. Their half-recovery times, $\tau_{1/2}$, were around 100 ms, which was slow enough for the time resolution of our image recording (5 ms). Since the diameter of the flagellum is extremely small (~0.2 μm) compared with that of the bleached area (~6 μm), it is reasonable to consider the recovery curves of fluorescence as the results of simple one-dimensional diffusion. Determined diffusion coefficients of these fluorescence probes in flagella, D_{fl}, were 64, 64 and 63 $\mu m^2 s^{-1}$ for calcein (M_r, 622.54), carboxyfluorescein (M_r, 376.32) and Oregon Green (M_r, 412.30), respectively (Table 1).

FRAP in aqueous solution

We also determined the diffusion coefficients of these fluorescent probes in aqueous solutions in order to test the accuracy of our measuring system and to compare them with diffusion coefficients in flagella. In each experiment, a 4 μl solution of fluorescence probe was put between the two glass coverslips to make a thin aqueous layer (estimated thickness ~7 μm). A small region in the thin aqueous layer was then photobleached by a laser pulse in a similar way to the measurements using sperm flagella. In contrast to flagella, the diffusion in this case should be regarded as occurring in two dimensions (Kao et al., 1993; Swaminathan et al., 1997). Also, since the fluorescent probes diffuse faster than the time resolution of our measuring system, we executed the experiment using various concentrations of glycerol (viscosity, 1.76–10.8 mPa s) to reduce the diffusion rates. Then, by extrapolating the results, we determined the diffusion coefficients at 1 mPa s as in aqueous solution without glycerol. A typical example of a fluorescence recovery curve in 20% glycerol solution (1.76 mPa s) is shown in Fig. 2D. Fig. 3 shows the relationship between diffusion rates and the viscosity of the solvent for each probe. As expected from the Einstein–Stokes equation, the reciprocal of the diffusion coefficient, $1/D$, varied proportionally with the viscosity of the medium. Diffusion coefficients for the probes in aqueous solution (viscosity, 1 mPa s), D_{aq}, were determined by extrapolating these data. As the measured diffusion coefficients tended to scatter at higher viscosities for unknown reasons, data at 10.8 mPa s were neglected for the least squares fitting, where we could assume the data were with uniform variances according to the White test ($P<0.01$) (White, 1980). D_{aq} was thus determined to be 337, 296 and 255 $\mu m^2 s^{-1}$ for calcein, carboxyfluorescein and Oregon Green, respectively (see Table 1).

The ratios of diffusion coefficients determined in flagella to those determined in solution, D_{fl}/D_{aq}, are also shown in Table 1. Diffusion coefficients we obtained were all lower in flagella compared to those in solution. The extent of the rate reductions varied slightly (0.19–0.25) depending on the species of probes.

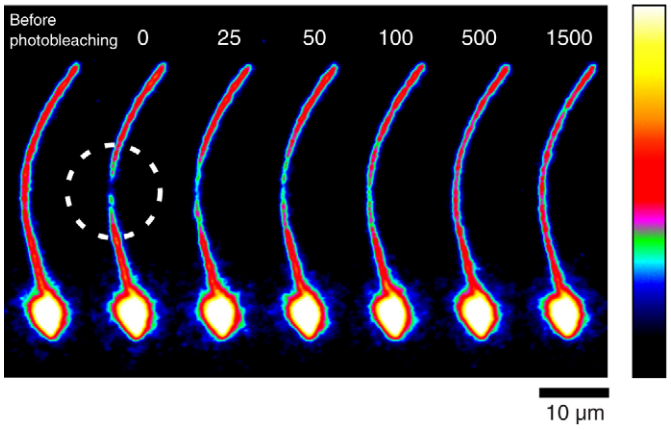

Fig. 1 Pseudo-color fluorescence images of calcein-loaded spermatozoa. Each image was obtained by averaging five frames (5 ms/frame). The resultant images of brightness maps are displayed in pseudo-color (white is the brightest and black is the faintest) to clarify the detail of photobleached area. The numbers shown above each image indicate the time course after the photobleaching laser pulse was applied (units: ms). The leftmost image was obtained just before photobleaching. The white circle indicates the region where the photobleaching laser pulse was directed. Scale bar, 10 μm.

Simulation of intraflagellar ATP diffusion

Simply assuming that the diffusion coefficient of ATP is similar to that of fluorescein derivatives of similar molecular masses (~60 $\mu m^2 s^{-1}$), the rate of ATP diffusion inside flagella is about three times lower than that expected in previous calculations (D ~150 $\mu m^2 s^{-1}$) by Tombes et al. (Tombes et al., 1987). In their model, ATP molecules are produced at the mitochondrion located at the proximal end of the flagellum and provided by diffusion, together with the ADP recycling system by creatine shuttle (Tombes and Shapiro, 1985). Using the same model, we simulated whether the energy could be sufficiently provided along the flagellum (length, 40 μm) when the parameter of the diffusion coefficient for ATP was set to 60 $\mu m^2 s^{-1}$ and the diffusion coefficients for other important molecules were set as shown in Table 2 and Fig. 4. We also calculated intraflagellar concentration profiles of ATP, ADP, AMP, creatine (Cr) and PCr. Effects of competitive inhibition of dynein ATPase activity by ADP as well as rate limiting effects of ADP recycling by the creatine shuttle were included. We could repeat the results that ATP concentration and dynein ATPase activity were high throughout the flagellum if the ATP diffusion coefficient of 150 $\mu m^2 s^{-1}$ was used, however, both gradually decreased at the tip of the flagellum when we used the diffusion coefficient of 60 $\mu m^2 s^{-1}$ (Fig. 4A,C). If we executed the same simulation in sperm flagella of 100 μm of length, we found energy supply was not enough at either rates of diffusion (60 or 150 $\mu m^2 s^{-1}$; Fig. 4B,D). In such a long flagellum, even if the ADP recycling system by the creatine shuttle is working, dynein ATPase activity is assumed to be significantly decreased at the distal portion of the flagellum at both diffusion rates,

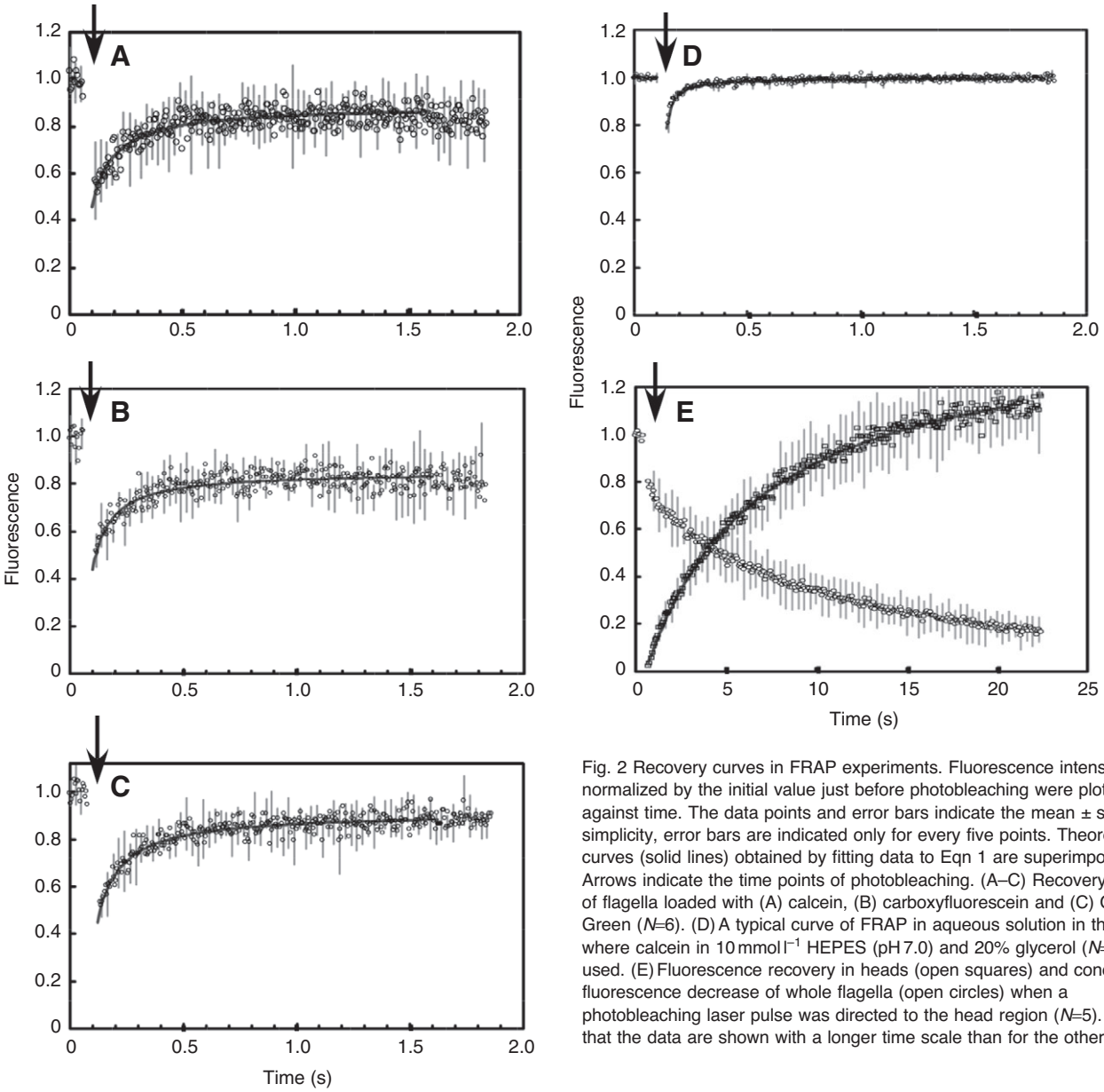

Fig. 2 Recovery curves in FRAP experiments. Fluorescence intensities normalized by the initial value just before photobleaching were plotted against time. The data points and error bars indicate the mean ± s.d. For simplicity, error bars are indicated only for every five points. Theoretical curves (solid lines) obtained by fitting data to Eqn 1 are superimposed. Arrows indicate the time points of photobleaching. (A–C) Recovery curves of flagella loaded with (A) calcein, (B) carboxyfluorescein and (C) Oregon Green (N=6). (D) A typical curve of FRAP in aqueous solution in the case where calcein in 10 mmol l^{-1} HEPES (pH 7.0) and 20% glycerol (N=3) was used. (E) Fluorescence recovery in heads (open squares) and concomitant fluorescence decrease of whole flagella (open circles) when a photobleaching laser pulse was directed to the head region (N=5). Note that the data are shown with a longer time scale than for the other four.

retarding flagellar beating as in the case of normal flagellar length (40 μm) with reduced creatine kinase activity (Tombes et al., 1987).

Diffusion between the head and flagellum

To investigate whether small probe molecules can go through the proximal basal-body region into the head, we directed a photobleaching pulse on the whole head region of a calcein-loaded spermatozoon. After bleaching, we observed gradual recovery of head fluorescence along with concomitant decrease in flagellar fluorescence signals (Fig. 2E). The half-recovery time, $\tau_{1/2}$, was 6.8±1.5 s (N=5), which was more than 60 times longer comparing with that of intraflagellar FRAP. Since there was no detectable change in the total amount of calcein molecules in the whole spermatozoon during the recovery, it is likely that we observed the slow diffusion of fluorescent probes from flagella to heads. Using Eqn 4 (see the Appendix as well), we determined the head/flagellum volume ratio of spaces where calcein can diffuse. The determined volume ratio, $V_{head}/V_{flagellum}$ was 4.6±1.9 (N=5).

DISCUSSION

We successfully determined the diffusion coefficients of fluorescent probes using fluorescein derivatives (calcein, carboxyfluorescein and Oregon Green) both in flagella (D_{fl}) and in aqueous solution (D_{aq}). The current work is the first to determine the rate of intra-flagellar diffusion. Diffusion coefficients of fluorescein-derived probes in aqueous solutions have been reported previously, but they ranged

Table 1. Diffusion coefficients

Probe dye	D_{fl}	D_{aq}	D_{fl}/D_{aq}
Calcein	64±28	337±129	0.19
Carboxyfluorescein	64±35	296±85	0.22
Oregon green	63±23	255±44	0.25

Determined diffusion coefficients (μm^2 s^{-1}) for each probe in flagella (D_{fl}) and aqueous solution (D_{aq}). D_{fl} values are means ± s.d. (N=6). D_{aq} values were determined by extrapolating the plots as in Fig. 3 (N=3, see the text for more details). The ratios, D_{fl}/D_{aq}, are also shown.

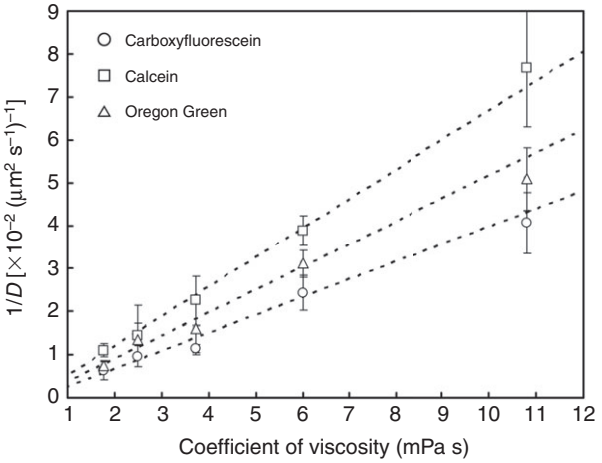

Fig. 3 Diffusion coefficients in aqueous solutions of various viscosity. Reciprocals of obtained diffusion coefficients *versus* viscosity. As expected from the Einstein–Stokes equation, they were linear relationships. The results of least-squares linear regression are shown by the broken lines. For the regression, data points at 10.8 mPa s were eliminated (see text for detail). The data points and error bars indicate the mean ± s.d. (N=3).

from ~150 to ~500 $\mu m^2 s^{-1}$ (Brown et al., 1999; Culbertson et al., 2002; Mustafa et al., 1993; Politz et al., 1998). Such a large variation was most probably the result of the differences in measuring methods or conditions rather than the differences in probe properties (e.g. molecular mass, shapes or charges). The D_{aq} values we obtained in this study were 337, 296 and 255 $\mu m^2 s^{-1}$ for calcein, carboxyfluorescein and Oregon Green, respectively (Table 1). All of these D_{aq} values were comparable to those previously reported, thus, confirming the accuracy of FRAP analysis by our system.

The ratios, D_{fl}/D_{aq}, were 0.19, 0.22 and 0.25 for calcein, carboxyfluorescein and Oregon Green, respectively (Table 1). One of the possible explanations for these ~80% reductions of D_{fl} relative to D_{aq} is that electrostatic interactions with the crowded components of axoneme attenuated the apparent D_{fl}. Another possibility, that these probes might be attached to intra-flagellar macromolecules that diffuse slowly, could not be fully excluded under our experimental conditions, so the values we obtained could reflect apparent diffusion rates affected by such macromolecules, if any, as well as by intra-flagellar viscosity and crowded effects. Our observation suggests that molecular mobility inside sperm cells would not simply depend on diffusion by random walk but on some interactions with intra-flagellar components, although whether it is specific or non-specific is unclear at present. Alternatively, the reduction of D_{fl} may be due to the restricted aqueous volume in the flagella where the cross section is mostly filled with axonemal structures. In mammalian nerve cells, diffusion coefficients of the Ca^{2+}-binding protein parvalbumin and fluorescein-labeled dextran have been reported to be ~10 $\mu m^2 s^{-1}$ in both axonal and somatic cytoplasm, but ~40 $\mu m^2 s^{-1}$ in dendrites (Schmidt et al., 2007), suggesting that, instead of cell shapes, molecular interaction with intracellular components would be the major factor reducing intracellular diffusional mobility. This could also be the case in sperm flagella. Further detailed investigations are required to determine the major factors in the reduction of diffusion coefficients in flagella.

Table 2. Diffusion coefficients used for the simulation

Molecular species	M_r	Tombes et al. (1987)	Present paper
ATP	507.18	150	60
ADP	428.21	150	60
AMP	349.24	150	60
PCr	211.11	260	104
Cr	131.12	260	104

Diffusion coefficients ($\mu m^2 s^{-1}$) for important molecules used in previous (Tombes et al., 1987) and the present simulations. As previously calculated, diffusion coefficients of ADP and AMP were regarded as identical to that of ATP, since their relative molecular masses (M_r) are close to each other. Also, the diffusion coefficient of phosphocreatine (PCr) was regarded as identical to that of creatine (Cr). As the diffusion coefficient for ATP was set to 60 $\mu m^2 s^{-1}$ (40% of that in the previous calculation), the diffusion coefficients for Cr and PCr were similarly set to 40% of the values used previously.

In the case of sea-urchin sperm flagella, the only energy source for flagellar motility is mitochondria located near the proximal ends. It has been described that an additional energy transferring system known as the 'creatine shuttle' is also present in sea urchin sperm (Tombes and Shapiro, 1985). By simulating the rates of ATP consumption and supply by diffusion of ATP and PCr, Tombes et al. (Tombes et al., 1987) concluded that enough ATP could only be provided from mitochondria to a flagellar tip when the creatine shuttle system is working. However, in their calculations, they used a diffusion coefficient for ATP of 150 $\mu m^2 s^{-1}$, which was indirectly obtained from the recovery rates of contraction force in muscle fibers (Bowen and Martin, 1963), as no appropriate data for diffusion coefficients in flagella was available. In the current work, we determined D_{fl} for three fluorescent probes to be ~60 $\mu m^2 s^{-1}$ which is about one third of that in muscle fibers (>150 $\mu m^2 s^{-1}$). Here, we again similarly calculated ATP diffusion by assuming D_{fl} of ATP and PCr to be 60 and 104 $\mu m^2 s^{-1}$, respectively (Table 2). It was revealed that ATP concentration gradually decreases toward the tip (Fig. 4A). However, even at the tip (40 μm from the proximal end of flagellum), ATP concentration was still maintained at more than 2 $mmol\,l^{-1}$ if the ATP concentration at the proximal end was as high as 6 $mmol\,l^{-1}$ and if the creatine shuttle system is working. This ATP concentration, even at the distal ends, would be high enough for the full activation of flagellar ATPases and bending motions, which have a K_m of about 100 $\mu mol\,l^{-1}$ (Gibbons and Gibbons, 1972). Even if there was competitive inhibition of dynein ATPase activity by accumulated ADP (Okuno and Brokaw, 1979), ATPase activity should still be kept high enough to sustain flagellar beating (Fig. 4C). Therefore, even if diffusion rates are three times smaller than those in muscle fibers, sea urchin sperm flagella with a creatine shuttle system could maintain continuous beating.

Using the same diffusion parameters, we also calculated the length limit of flagella (Fig. 4B,D). In the case with a flagellum longer than 60 μm, the tip concentration of ATP was estimated to be lower than 100 $\mu mol\,l^{-1}$ (Fig. 4B,D), a problematic concentration to maintain regular beating. Even if the diffusion coefficients of ATP and PCr are 150 and 260 $\mu m^2 s^{-1}$, respectively (Table 2), the maximum possible length of a flagellum is 100 μm in this model (Fig. 4B). Dynein ATPase activities seem to be significantly decreased in both cases (Fig. 4B,D). In many other cases, the flagella of mammalian spermatozoa are longer than this (e.g. ~150 μm for mouse spermatozoa) and our calculation indicates that a simple diffusion pathway by itself cannot provide full energy for flagellar movements. Indeed, unlike sea urchin spermatozoa, it has been reported that mammalian sperm have glycolytic enzymes in the tail

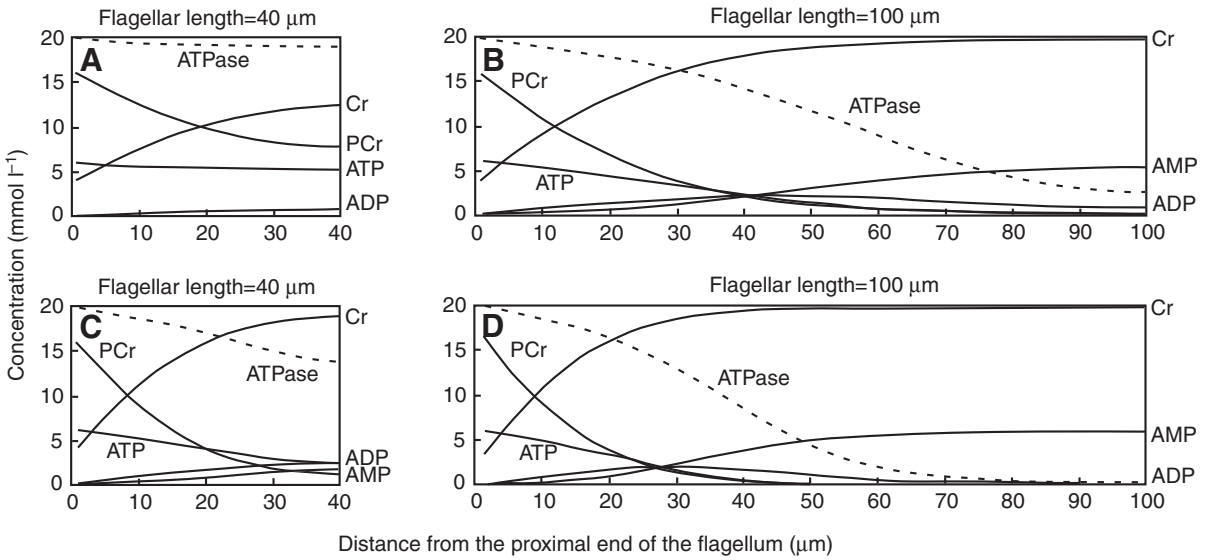

Fig. 4. Simulated profiles of the concentrations of intraflagellar materials (solid lines) and dynein ATPase activity (broken lines; relative values) along flagella. The simulation was executed based on the model by Tombes et al. (Tombes et al., 1987). The lengths of flagella were set to 40 μm (A,C) and 100 μm (B,D). The ATP diffusion coefficients of 150 (A,B) and 60 $\mu m^2 s^{-1}$ (C,D) were used. The diffusion coefficients of other molecules are shown in Table 2. In A and B, where we used D=150 $\mu m^2 s^{-1}$, we obtained almost the same results as those previously reported by Tombes et al. (Tombes et al., 1987).

region and this metabolic pathway may play the major role in providing ATP (Mukai and Okuno, 2004). Without such a system providing ATP, flagella longer than 60 μm, as in the case of other invertebrate spermatozoa and dinoflagellates, for example, could solve the problem by other means. For example, making flagellar diameter larger so as to produce larger diffusion channels, reducing intarcellular obstacles to ATP mobility, or beating with lower frequency and smaller bend amplitudes in order to save ATP consumption could be possible options. An active ATP/PCr transport system along flagella might be a possible solution, although we have no evidence so far.

We were also interested in the material diffusion through the neck region since specific structures in the basal body region, including membrane necklace-like structures, could be working as diffusion barriers. Electron microscopy analyses have shown that the proximal ends of flagella of mammalian spermatozoa (Pessh and Bergmann, 2006) and an alga, *Chlamydomonas reinhardtii* (Mitchell et al., 2005), are densely packed, which may restrict the diffusivity and would be possible candidates as diffusion barriers between flagella and heads (or cell bodies). These structural obstacles may function generally as diffusion barriers in other types of eukaryotic cilia and flagella. Therefore, the active intra-flagellar transport (IFT) must be a vital system in forming the structure and maintaining the functions of cilia and flagella in many cases (Bisgrove and Yost, 2006; Rosenbaum and Witman, 2002). In similar FRAP experiments with calcein, we observed fluorescence recovery in the head region (Fig. 2E). We found head fluorescence recovery, with a half-recovery time ($\tau_{1/2}$) of 6.8±1.5 s (N=5), indicating calcein could move between head and flagellar regions. Note that in flagella, $\tau_{1/2}$ was around 100 ms; thus, the fluorescence recovery rate was more than 60 times slower in the head than in the flagellum. Unlike the cylindrical shape of flagellum, the head spreads three-dimensionally and it is difficult to simply compare the FRAP rates between the head and flagellum. However, the apparent diffusion rate at the neck region was obviously lower than that in the tail region, suggesting the presence of a diffusion barrier around the neck region of spermatozoa. It is currently not clear whether the barrier is on the head side or flagellar side of the mitochondrion, or whether the mitochondrion itself would be a structural barrier for diffusion. If diffusion is restricted between mitochondrial and tail regions, some mechanism, such as a molecular filter, should exist to move molecules such as ATP or PCr from the mitochondrion to the flagellum, although this requires further investigation. How the diffusion barrier between head and flagellum, if present, can be generalized to other cells and how the IFT system is compromising or co-operating with the diffusion hurdles remain to be clarified.

From the data obtained from the FRAP experiments of heads, we next estimated $V_{head}/V_{flagellum}$, the ratio of head/flagellum volume of the space that calcein molecules can access. The obtained value of $V_{head}/V_{flagellum}$ was 4.6±1.9, corresponding to 82% of the volume of the head and 18% of the flagellum. If we assume that a sperm head is a sphere with a diameter of 3.8 μm and the flagellum is a cylinder of 0.2 μm diameter and 40 μm length, then $V_{head}/V_{flagellum}$ is estimated to be 23. Thus, the morphologically estimated volume percentages are 96% for head and 4% for flagellum. The value we obtained is reasonable because the structural components inside heads, such as DNA and acrosomes that are essential for fertilization and reproductions, are expected to be packed tightly, that is, heads are not simple, empty spheres.

In our current work, apparent diffusion coefficients for fluorescein-derived probes in flagella were determined and it was confirmed that calcein molecules can diffuse between the head and the flagellum. Our FRAP experimental system can, in principle, be applied to determine the diffusion coefficients even in motile flagella. Along with the analysis of the diffusion of macromolecules such as dextran-conjugated dyes or GFP, we expect that we will be able to clarify more detailed features of molecular diffusion and, thus, energy and material transportation in flagella as well as the biological significance of intra-spermatozoa compartmentalization.

This work was supported by the program of Creation and Application of Soft Nano-Machine, the Hyperfunctional Molecular Machine (CREST, JST), and by a Grant-in-Aid for Scientific Research on Priority Areas (no. 1704911, no. 19037010). The authors are grateful to the Misaki Marine Biological Station, the University of Tokyo for supplying sea urchins.

APPENDIX

Estimation of head/flagellum volume ratio

After the head areas of the spermatozoa were photobleached, gradual fluorescence recovery with a low time constant ($\tau_{1/2}$ ~7 s) was observed as well as the concomitant decrease of fluorescence in the tail region. Such observations led us to estimate the ratio of head/flagellum volume as follows.

When the sperm head was photobleached, the total amount of fluorescent probe in the tail region, S_{f0} (at t=0), is given by:

$$S_{f0} = C_{f0}V_{flagellum} , \quad (A1)$$

where C_{f0} is the concentration of remaining fluorescent probe in the flagellar region, and $V_{flagellum}$ is the volume of flagellar intracellular space that fluorescent molecules can freely access. Similarly, the total amount of fluorescent probe in the head, S_{h0}, is expressed as:

$$S_{h0} = C_{h0}V_{head} + C_{a0}V_{acrosome} + C_{m0}V_{mitochondrion} , \quad (A2)$$

where C_{h0}, C_{a0} and C_{m0} are the concentrations of probes at t=0 in the head, acrosome and mitochondrion, respectively, and V_{head}, $V_{acrosome}$ and $V_{mitochondrion}$ are the volumes of spaces where probes can be incorporated in the head, acrosome and mitochondrion, respectively.

After fluorescence in the head area is finally recovered (at t=∞), the total amounts of fluorescence probe in the flagellum ($S_{f\infty}$) and in the head ($S_{h\infty}$) are expressed by:

$$S_{f\infty} = C_{f\infty}V_{flagellum} , \quad (A3)$$

$$S_{h\infty} = C_{h\infty}V_{head} + C_{a\infty}V_{acrosome} + C_{m\infty}V_{mitochondrion} , \quad (A4)$$

where $C_{f\infty}$, $C_{h\infty}$, $C_{a\infty}$ and $C_{m\infty}$ are the final concentrations of fluorescent probes (at t=∞) in the flagellum, head, acrosome and mitochondrion, respectively. If all the fluorescence recovery in the head region is by probe diffusion from the flagellum:

$$S_{f0} - S_{f\infty} = S_{h\infty} - S_{h0} . \quad (A5)$$

Given that probe concentrations both in the acrosome and mitochondrion regions are kept constant by membranous compartmentalization (i.e. no transfer of probe between cytoplasm and such organelles occurs), from Eqns A1–A5 we obtain:

$$(C_{f0} - C_{f\infty})V_{flagellum} = (C_{h\infty} - C_{h0})V_{head} .$$

Thus,

$$V_{head} / V_{flagellum} = (C_{f0} - C_{f\infty}) / (C_{h\infty} - C_{h0}) . \quad (A6)$$

If $C_{f\infty}$ and $C_{h\infty}$ are equal at t=∞, Eqn A6 can be transformed into:

$$V_{head} / V_{flagellum} = (C_{f0} / C_{f\infty} - 1) / (1 - C_{h0} / C_{h\infty}) . \quad (A7)$$

Since fluorescence intensities are generally proportional to the concentrations of fluorescent probes when the volumes of solutions are the same, we can expect:

$$C_{f0} / C_{f\infty} = F_{f0} / C_{f\infty} , \quad (A8)$$

$$C_{h0} / C_{h\infty} = F_{h0} / C_{h\infty} , \quad (A9)$$

where F_{f0} and $F_{f\infty}$ are the observed intensities of total fluorescence in the flagellum at t=0 and t=∞, respectively, and F_{h0} and $F_{h\infty}$ are those in the head. Thus, from Eqns A7–A9, the volume ratio is determined by the following equation:

$$V_{head} / V_{flagellum} = (F_{f0} / F_{f\infty} - 1) / (1 - F_{h0} / F_{h\infty}) .$$

This final equation is the same as Eqn 4 in Materials and methods.

REFERENCES

Bisgrove, B. W. and Yost, H. J. (2006). The roles of cilia in developmental disorders and disease. *Development* **133**, 4131-4143.
Bowen, W. J. and Martin, H. L. (1963). A study of diffusion of ATP through glycerol-treated muscle. *Arch. Biochem. Biopys.* **102**, 286-292.
Brokaw, C. J. (1966). Mechanics and energetics of cilia. *Am. Rev. Respir. Dis.* **93**, 32-40.
Brown, E. B., Wu, E. S., Zipfel, W. and Webb, W. W. (1999). Measurement of molecular diffusion in solution by multiphoton fluorescence photobleaching recovery. *Biophys. J.* **77**, 2837-2849.
Culbertson, C. T., Jacobson, S. C. and Ramsey, J. M. (2002). Diffusion coefficient measurements in microfluidic devices. *Talanta* **56**, 365-373.
Darszon, A., Beltran, C., Felix, R., Nishigaki, T. and Trevino, C. L. (2001). Review: Ion transport in sperm signaling. *Dev. Biol.* **240**, 1-14.
Gibbons, B. H. and Gibbons, I. R. (1972). Flagellar movement and adenosine triphosphatase activity in sea urchin sperm extracted with Triton X-100. *J. Cell Biol.* **54**, 75-97.
James, P. S., Hennessy, C., Berge, T. and Jones, R. (2004). Compartmentalization of the sperm plasma membrane: a FRAP, FLIP and SPFI analysis of putative diffusion barriers on the sperm head. *J. Cell Sci.* **117**, 6485-6495.
Kao, H. P., Abney, J. R. and Verkman, A. S. (1993). Determination of the translational mobility of a small solute in cell cytoplasm. *J. Cell Biol.* **120**, 175-184.
Ladha, S., Mackie, A. R. and Clark, D. C. (1994). Cheek cell membrane fluidity measured by fluorescence recovery after photobleaching and steady-state fluorescence anisotropy. *J. Membr. Biol.* **142**, 223-228.
Ladha, S., James, P. S., Clark, D. C., Howes, E. A. and Jones, R. (1997). Lateral mobility of plasma membrane lipids in bull spermatozoa: heterogeneity between surface domains and rigidification following cell death. *J. Cell Sci.* **110**, 1041-1050.
Mackie, A. R., James, P. S., Ladha, S. and Jones, R. (2001). Diffusion barriers in ram and boar sperm plasma membranes: directionality of lipid diffusion across the posterior ring. *Biol. Reprod.* **64**, 113-119.
Mitchell, B. F., Pedersen, L. B., Feely, M., Rosenbaum, J. L. and Mitchell, D. R. (2005). ATP production in *Chlamydomonas reinhardtii* flagella by glycolytic enzymes. *Mol. Biol. Cell* **16**, 4509-4518.
Mukai, C. and Okuno, M. (2004). Glycolysis plays a major role for adenosine triphosphate supplementation in mouse sperm flagellar movement. *Biol. Reprod.* **71**, 540-547.
Mustafa, M. B., Tipton, D. L., Barkley, M. D., Ruaso, P. S. and Blum, F. D. (1993). Dye diffusion in isotropic and liquid crystalline aqueous (hydroxypropy1) cellulose. *Macromolecules* **26**, 370-378.
Nevo, A. C. and Rikmenspoel, R. (1970). Diffusion of ATP in sperm flagella. *J. Theor. Biol.* **26**, 11-18.
Nicastro, D., McIntosh, J. R. and Baumeister, W. (2005). 3D structure of eukaryotic flagella in a quiescent state revealed by cryo-electron tomography. *Proc. Natl. Acad. Sci. USA* **102**, 15889-15894.
Okuno, M. and Brokaw, C. J. (1979). Inhibition of movement of Triton-demembranated sea urchin sperm flagella by Mg^{2+}, ATP^{4-}, ADP and P_i. *J. Cell Sci.* **38**, 105-123.
Pessh, S. and Bergmann, M. (2006). Review: structure of mammalian spermatozoa in respect to viability, fertility and cryopreservation. *Micron* **37**, 597-612.
Politz, J. C., Browne, E. S., Wolf, D. E. and Pederson, T. (1998). Intranuclear diffusion and hybridization state of oligonucleotides measured by fluorescence correlation spectroscopy in living cells. *Proc. Natl. Acad. Sci. USA* **95**, 6043-6048.
Rodriguez, E. and Darszon, A. (2003). Intracellular sodium changes during the speract response and the acrosome reaction in sea urchin sperm. *J. Physiol.* **546**, 89-100.
Rosenbaum, J. L. and Witman, G. B. (2002). Intraflagellar transport. *Nat. Rev. Mol. Cell. Biol.* **3**, 813-825.
Schmidt, H., Arendt, O., Brown, E. B., Schwaller, B. and Eilers, J. (2007). Parvalbumin is freely mobile in axons, somata and nuclei of cerebellar Purkinje neurons. *J. Neurochem.* **100**, 727-735.
Swaminathan, R., Hoang, C. P. and Verkman, A. S. (1997). Photobleaching recovery and anisotropy decay of green fluorescent protein GFP-S65T in solution and cells: cytoplasmic viscosity probed by green fluorescent protein translational and rotational diffusion. *Biophys. J.* **72**, 1900-1907.
Tombes, R. M. and Shapiro, B. M. (1985). Metabolite channeling: a phosphorylcreatine shuttle to mediate high energy phosphate transport between sperm mitochondrion and tail. *Cell* **41**, 325-334.
Tombes, R. M., Brokaw, C. J. and Shapiro, B. M. (1987). Creatine kinase-dependent energy transport in sea urchin spermatozoa. *Biophys. J.* **52**, 75-86.
Wey, C. L. and Cone, R. A. (1981). Lateral diffusion of rhodopsin in photoreceptor cells measured by fluorescence photobleaching and recovery. *Biophys. J.* **33**, 225-232.
White, H. (1980). A heteroskedasticity-consistent covariance matrix estimator and a direct test for heteroskedasticity. *Econometrica* **48**, 817-838.
Yguerabide, J., Schmidt, J. A. and Yguerabide, E. E. (1982). Lateral mobility in membranes as detected by fluorescence recovery after photobleaching. *Biophys. J.* **40**, 69-75.